Electrochemical Impedance Spectroscopy of Polyelectrolyte Multilayer Modified Gold Electrodes: Influence of Supporting Electrolyte and Temperature

ARTICLE *in* LANGMUIR · SEPTEMBER 2005

Impact Factor: 4.46 · DOI: 10.1021/la0507176 · Source: PubMed

5 AUTHORS, INCLUDING:

Tiago Henriques Silva
University of Minho
33 PUBLICATIONS **236** CITATIONS
SEE PROFILE

Vladimir García-Morales
University of Valencia
41 PUBLICATIONS **580** CITATIONS
SEE PROFILE

José A. Manzanares
University of Valencia
116 PUBLICATIONS **2,038** CITATIONS
SEE PROFILE

A Fernando Sousa Silva
University of Porto
162 PUBLICATIONS **2,203** CITATIONS
SEE PROFILE

Electrochemical Impedance Spectroscopy of Polyelectrolyte Multilayer Modified Gold Electrodes: Influence of Supporting Electrolyte and Temperature

Tiago H. Silva,*,† Vladimir Garcia-Morales,‡ Cosme Moura,† José A. Manzanares,‡ and Fernando Silva†

LEQA, Laboratório de Electroquímica e Química Analítica, CIQ-L4 Departamento de Química, Faculdade de Ciências do Porto, Rua do Campo Alegre 687, 4169-007 Porto, Portugal and Departament de Termodinàmica, Universitat de València, C/Dr. Moliner 50, E-46100 Burjassot, Spain

Received March 17, 2005. In Final Form: May 6, 2005

Electrochemical impedance spectroscopy and cyclic voltammetry are employed to characterize poly(styrenesulfonate)/poly(allylamine hydrochloride) multilayers assembled onto cysteamine-modified gold surfaces. The influence of the supporting electrolyte and temperature on the impedance response is studied because of both its practical interest and the need to test further the capillary membrane model recently developed by Barreira et al. [*J. Phys. Chem. B* **2004**, *108*, 17973]. The results obtained are interpreted quite satisfactorily in terms of this model, thus providing additional support to its usefulness for the description of ionic transport through polyelectrolyte multilayers. It is observed that the nature of the supporting electrolyte affects the film resistance and the electrode coverage. The temperature dependence of the diffusion coefficient is shown to follow the Arrhenius law, and the activation energy is estimated as 61 kJ/mol. Experiments with a large number of layers are also included to show that the impedance response of the multilayer then resembles that of a homogeneous membrane.

1. Introduction

Polyelectrolyte multilayers (PEMUs) are a new kind of materials promising applications in different fields such as separation membranes,[1−3] drug delivery,[4,5] and sensors.[6,7] PEMUs are built up by alternating adsorption of anionic and cationic polyelectrolytes from aqueous solutions and represent a step forward in the development of surface chemistry.[8,9] Sensors can be prepared by the incorporation of reactant species into the multilayer through substitutional deposition,[6,9] chemical modification,[6,8] and "infiltration" into the preassembled multilayer.[7] The properties of the electrochemical sensors thus prepared depend largely on how sensitively the thin films recognize target analytes and how rapidly they communicate the resulting signals to the underlying electrode. Therefore, for the success in their development, it is mandatory to investigate the interaction of the film with the analyte and the kinetics of charge and mass transport through the film.[10]

The stability of PEMUs is linked to a mechanism of charge compensation through complexation of the polyelectrolyte chains, leading to an entangled structure (the so-called intrinsic compensation[11]). When the multilayer is immersed in an electrolyte solution, small mobile ions enter the structure and participate in the charge compensation (the so-called extrinsic compensation[11]). Moreover, these ions carry solvent molecules, causing the swelling of the structure. The properties of the multilayer and, specifically, their permeability to ions and molecules, which is a key issue in the practical application of polyelectrolyte multilayered films, depend on the degree of swelling and on the existence of pores or structural defects.

The multilayer structure may also be affected by environmental conditions[4,12−20] such as ionic strength and temperature, and there is still some controversy as to whether[5,11,16] or not[15] the addition of salt affects the structure after preparation. Although several studies have been carried out on the relationship between structure and experimental conditions during multilayer preparation, much less attention has been paid to the eventual change of that structure after preparation.[5,15]

* Author to whom correspondence should be addressed. E-mail: thsilva@fc.up.pt. Telephone: (351) 22 6082919. Fax: (351) 22 6082959.

† LEQA, Laboratório de Electroquímica e Química Analítica.

‡ Universitat de València.

(1) Krasemann, L.; Tieke, B. *Langmuir* **2000**, *16*, 287.
(2) Toutianoush A.; Tieke, B. *Mater. Sci. Eng., C* **2002**, *22*, 135.
(3) Bruening, M. L.; Sullivan, D. M. *Chem.—Eur. J.* **2002**, *8*, 3833.
(4) Antipov, A. A.; Sukhorukov, G. B.; Mohwald, H. *Langmuir* **2003**, *19*, 2444.
(5) Gao, C. Y.; Leporatti, S.; Moya, S.; Donath, E.; Mohwald, H. *Chem.—Eur. J.* **2003**, *9*, 915.
(6) Lee, S. H.; Kumar, J.; Tripathy, S. K. *Langmuir* **2000**, *16*, 10482.
(7) Yu, A. M.; Liang, Z. J.; Cho, J. H.; Caruso, F. *Nano Lett.* **2003**, *3*, 1203.
(8) Barreira, S. V. P.; Silva F. *Langmuir* **2003**, *19*, 10324.
(9) Caruso, F.; Niikura, K.; Furlong, D. N.; Okahata, Y. *Langmuir* **1997**, *13*, 3427.
(10) Komura, T.; Yamaguchi, T.; Shimatani, H.; Okushio, R. *Electrochim. Acta* **2004**, *49*, 597.
(11) Schlenoff, J. B.; Ly, H.; Li, M. *J. Am. Chem. Soc.* **1998**, *120*, 7626.
(12) Steitz, R.; Jaeger, W.; von Klitzing, R. *Langmuir* **2001**, *17*, 4471.
(13) Dubas, S. T.; Schlenoff, J. B. *Macromolecules* **1999**, *32*, 8153.
(14) Tan, H. L.; McMurdo, M. J.; Pan, G. Q.; Van Patten, P. G. *Langmuir* **2003**, *19*, 9311.
(15) Steitz, R.; Leiner, V.; Siebrecht, R.; von Klitzing, R. *Colloids Surf., A* **2000**, *163*, 63.
(16) Dubas, S. T.; Schlenoff, J. B. *Macromolecules* **2001**, *34*, 3736.
(17) Silva, T. H.; Barreira, S. V. P.; Moura, C.; Silva, F. *Port. Electrochim. Acta* **2003**, *21*, 281.
(18) Garcia-Morales, V.; Silva, T. H.; Moura, C.; Manzanares, J. A.; Silva, F. *J. Electroanal. Chem.* **2004**, *569*, 111.
(19) Barreira, S. V. P.; Garcia-Morales, V.; Pereira, C. M.; Manzanares, J. A.; Silva, F. *J. Phys. Chem. B* **2004**, *108*, 17973.
(20) Harris J. J.; Bruening, M. L. *Langmuir* **2000**, *16*, 2006.

10.1021/la0507176 CCC: $30.25
Published on Web 06/24/2005

Most transport studies of PEMUs have employed sodium chloride as the supporting electrolyte,[4,16,20,21] but our previous work[18] has evidenced that the nature of the supporting electrolyte is worth a more thorough consideration. When the supporting electrolyte ions are multivalent, Donnan exclusion/inclusion phenomena have a major influence on the permeability.[1,18,22] When the charge numbers of the supporting electrolyte ions are small in magnitude, it is the thickness of the multilayer and the diffusivity that rules the permeability of the electroactive species.

In this paper, we use electrochemical impedance spectroscopy (EIS) and cyclic voltammetry (CV) to study the permeability of poly(styrene sulfonate)/poly(allylamine hydrochloride) (PSS/PAH) multilayers with different numbers of layers to the electrochemical probe $[Fe(CN)_6]^{3-/4-}$. Ellipsometry was used to assess the thickness of the multilayered films. EIS has been used with success to study the structure and transport properties of different films, either monolayers[10,23,24] or polyelectrolyte multilayers,[19,20,25−27] adsorbed on the surface of an electrode. This technique allows the gaining of insight into the effects of solution resistance, double-layer charging, and currents attributable to diffusion or to other processes occurring in the film.[24,28] We are interested in extending previous studies on PSS/PAH multilayers[17−20] to determine the influence of the nature of the supporting electrolyte and the temperature on the permeability because of both its practical importance and the convenience to test further the capillary membrane model (CMM) proposed in Ref 19. This theoretical model was developed to account for the transport properties of PEMUs at different stages of growth and describes the multilayer deposited on the electrode as a porous film with circular uncovered spots (or pinholes) that decrease in size and number as the number of layers increases. This model accounts satisfactorily for the experimental trends observed in CV and EIS measurements and allows us to determine structural parameters such as the effective electrode coverage and the radius of the active areas, in addition to transport parameters such as the effective diffusion coefficient of the electroactive species in the multilayer.

2. Experimental Section

Materials. Cysteamine (Fluka), PSS = poly(sodium 4-styrenesulfonate) (MW = 70 000, Aldrich), PAH = poly(allylamine hydrochloride) (MW = 15 000, Aldrich), supporting electrolytes $NaClO_4 \cdot H_2O$ (Merck), $KClO_4$ (Merck), $Ca(ClO_4)_2 \cdot 4H_2O$ (Aldrich), $Ba(ClO_4)_2$ (Aldrich), $La(ClO_4)_3$ (40 wt % solution in water) (Aldrich), and electrochemical probes $K_4[Fe(CN)_6] \cdot 3H_2O$ (Fluka) and $K_3[Fe(CN)_6]$ (Merck) were all used without further purification. Ultrapure water (18 MΩ cm, Millipore) was used in all experiments and cleaning procedures.

Methodology. Gold disk electrodes were polished with a polishing cloth (Buehler), rinsed with water, and then cleaned by cycling between the potentials −0.3 and 1.5 V vs Ag/AgCl in 0.1 M $HClO_4$ solution at a scan rate of 100 mV s^{-1} until reproducible scans were recorded (1 h approximately). Finally, the electrodes were rinsed with water and ethanol. The clean electrodes were immersed in a 3 mM cysteamine ethanolic solution overnight for approximately 14−16 h. They were then rinsed with ethanol, followed by water. The first polyelectrolyte multilayer was deposited onto a cysteamine-modified electrode from aqueous 0.1 M acetate buffer solution, pH = 4.5, containing 1 mg mL^{-1} of PSS for 20 min and then rinsed with water for 1 min. This procedure was repeated either using PSS or PAH to produce the desired number of layers. Multilayers with odd number of layers N were terminated with a PSS layer, while those with even N were terminated with a PAH layer.

Electrochemical Measurements. All electrochemical experiments were performed at room temperature (≈20 °C), unless otherwise specified, in a three-electrode cell containing a modified gold disk with a diameter of 2 mm (Radiometer EM-EDI-AuD2) as a working electrode, and a platinum net as a counter electrode. All potentials are reported against a Ag/AgCl/NaCl 3M reference electrode connected to the working volume with a Luggin capillary. The cell was enclosed in a grounded Faraday cage. Solutions filling the electrochemical cell were purged with nitrogen for 10 min before each measurement, and the cell was kept under flowing nitrogen for the duration of the experiment. For the systematic study of modified electrodes with a different number of polyelectrolyte layers, cyclic voltammograms were measured with the electrochemical cell filled with 0.5 M $NaClO_4$ and 1 mM $K_4Fe(CN)_6$ using an Autolab PSTAT 10 potentiostat. The potential was scanned between −0.2 and 0.6 V at 50 mV s^{-1}. EIS measurements were performed using a Solartron 1287 frequency response analyzer connected to a Solartron 1250 potentiostat in the frequency range 10^4−0.1 Hz. The electrochemical cell was then filled with 0.5 M $NaClO_4$, 1 mM $K_4Fe(CN)_6$, and 1 mM $K_3Fe(CN)_6$. The $[Fe(CN)_6]^{3-/4-}$ formal potential was chosen as the bias potential. All other electrochemical measurements were carried with the cell filled with 0.1 M supporting electrolyte, 1 mM $K_4Fe(CN)_6$, and 1 mM $K_3Fe(CN)_6$ using the Solartron equipment.

Ellipsometry. Polyelectrolyte films with three layer pairs were self-assembled on gold slides (5 nm Cr and 100 nm Au, Evaporated Metal Films), following the procedure described above. After preparation, they were left overnight immersed in a 0.1 M electrolyte ($NaNO_3$, KNO_3, $Ca(NO_3)_2$, or $Ba(NO_3)_2$) solution. After removal from the electrolyte solution and prior to all ellipsometric measurements, they were washed with water and dried in a stream of nitrogen. Ellipsometric measurements were obtained with an EP3 Nanofilm ellipsometer. The wavelength was 532 nm for all experiments. The thickness values of $(PSS + PAH)_3$ films were determined from the average of the measurements using three angles of incidence: 65°, 70°, and 75°. Substrate parameters (n = 0.4714 and k = 2.261) were measured after adsorption of cysteamine, ensuring that any changes in substrate reflectivity due to Au−S bonds will not affect subsequent measurements. A refractive index of 1.6 (and k = 0) was assumed for all films because they are not thick enough for refractive index determination.[20]

3. Theory

The capillary membrane model (CMM) considers that the electrode coverage is not complete in the early stages of growth of the multilayer and describes it as an array of circular areas that are uncovered by the polyelectrolytes and, therefore, more accessible to the electroactive species (see Figure 1a).[19] These uncovered electrode areas may persist during the sequential assembly of the polyelectrolyte layers, although progressively reduced in area and number as more layers are added. These areas play a key role in the transport properties of the multilayer even after they are completely covered because the film is less dense in those regions where there were opened spots previously, and the flux density of the electroactive species is higher there. This situation is depicted in Figure 1b. Finally, when the number of layers is large (ca. $N > 10$), the structure of the PEMU becomes very compact and

(21) Fery, A.; Scholer, B.; Cassagneau, T.; Caruso, F. *Langmuir* **2001**, *17*, 3779.
(22) Rubinstein, I.; Rubinstein, I. *J. Phys. Chem.* **1987**, *91*, 235.
(23) Cui, X. L.; Jiang, D. L.; Diao, P.; Li, J. X.; Tong, R. T.; Wang, X. K. *J. Electroanal. Chem.* **1999**, *470*, 9.
(24) Janek, R. P.; Fawcett, W. R.; Ulman A. *Langmuir* **1998**, *14*, 3011.
(25) Han S.; Lindholm-Sethson, B. *Electrochim. Acta* **1999**, *45*, 845.
(26) Pardo-Yissar, V.; Katz, E.; Lioubashevski, O.; Willner, I. *Langmuir* **2001**, *17*, 1110.
(27) Lindholm-Sethson, B. *Langmuir* **1996**, *12*, 3305.
(28) Bard A. J.; Faulkner, L. R. *Electrochemical Methods: Fundamentals and Applications*; Wiley: New York, 2001.

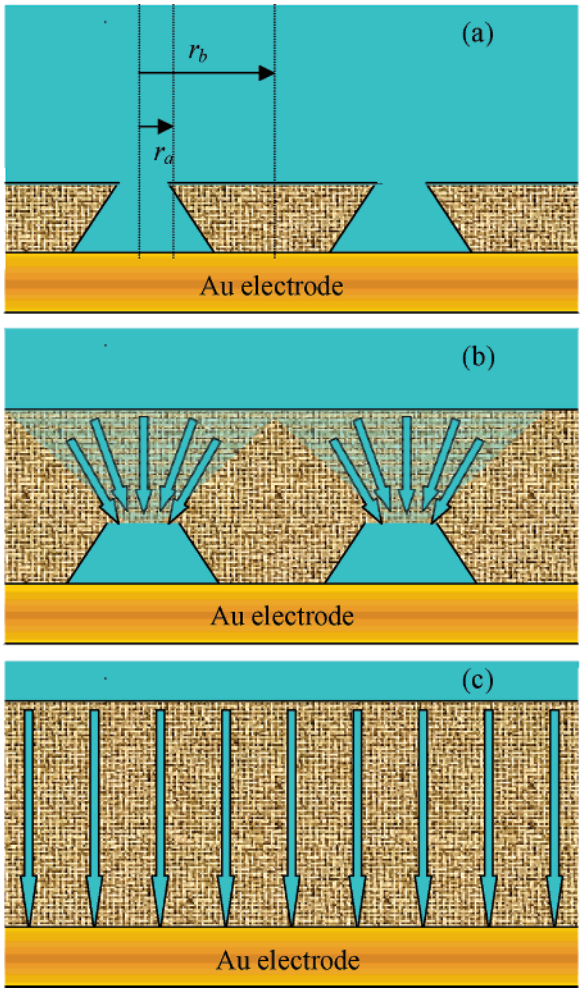

Figure 1. Diffusion paths (in blue) across the multilayer at three different stages of growth: (a) diffusion through open spots and capillaries at early stage, (b) diffusion through partially covered capillaries at moderate number of layers, and (c) homogeneous membrane limit when the number of layers is large.

practically homogeneous. This homogeneous membrane limit is depicted in Figure 1c.

The diffusion impedance of partially blocked electrodes used to fit the experimental results is explained in detail elsewhere (see ref 19 and references therein) and has the following form

$$Z_{\mathrm{d}}^{(c)} = \sum_k \frac{\sigma_k^{(c)}}{\sqrt{\omega}}\left[1 + \frac{\theta}{(1-\theta)}\left(\frac{[1+(q_k/\omega)^2]^{1/2} + q_k/\omega}{1+(q_k/\omega)^2}\right)^{1/2} + j + \frac{j\theta}{(1-\theta)}\left(\frac{[1+(q_k/\omega)^2]^{1/2} - q_k/\omega}{1+(q_k/\omega)^2}\right)^{1/2}\right] \quad (1)$$

where

$$\sigma_k^{(c)} = \frac{RT}{n^2F^2A\sqrt{2D_k^f\, c_k^f}} \quad (2)$$

and

$$q_k = \frac{D_k^f}{r_a^2}\begin{cases} \dfrac{2}{\theta \ln(1 + 0.27/\sqrt{1-\theta})} & 1-\theta > 0.1 \\ 2.78 & 1-\theta \le 0.1 \end{cases} \quad (3)$$

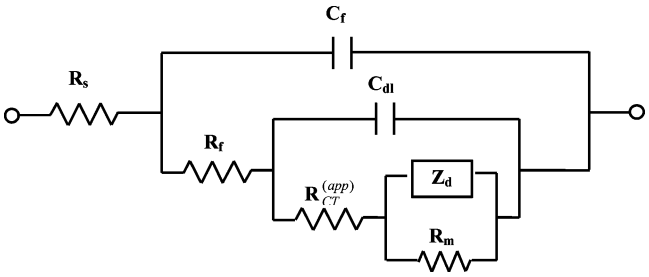

Figure 2. Equivalent circuit for the PEM-modified electrode where R_s is the solution resistance, C_f is the film capacitance, R_f is the film resistance, C_{dl} is the double-layer capacitance associated with the metal surface, $R_{CT}^{(app)}$ is the apparent charge-transfer resistance, R_m is the resistance representing ohmic conduction in the film, and Z_d is the diffusion impedance given by eq 1.

In eqs 1−3, k is an index for the electroactive species ($k = 1$ for $[Fe(CN)_6]^{4-}$ and $k = 2$ for $[Fe(CN)_6]^{3-}$), R is the gas constant, T is the temperature, F is the Faraday constant, n is the number of electrons involved in the electrode reaction ($n = 1$ in our case), A is the electrode area, j is $\sqrt{-1}$, and ω is the angular frequency. The coverage θ, the radius of the circular active areas r_a, and the radius r_b of inactive area surrounding the active site are related by the following equation

$$1 - \theta = \frac{r_a^2}{r_b^2} \quad (4)$$

Furthermore, because of the different nature of the paths as the coverage increases, the effective diffusion coefficient of species k in the multilayer, D_k^f, departs from that in the external solution, D_k^s, in a factor D_R, i.e., $D_k^f \equiv D_R D_k^s$. For the sake of simplicity, we take $D_1^s = D_2^s = D^s = 5.1 \times 10^{-6}$ cm^2 s^{-1}.

The CMM diffusion impedance is introduced in the equivalent circuit in Figure 2, which has been previously discussed and shown to account satisfactorily for the impedance spectra of several PEMUs.[19] The theoretical impedances for this equivalent circuit were calculated using Matlab. The fittings were monitored by plotting the real and imaginary parts of the impedance as well as the diffusion impedance. It is important to stress that, because of the complexity of the elements involved, the fittings were done by tentatively approaching the experimental curves through appropriate choices of the numerical values. The fittings were then refined by variation of the parameters and evaluation of the squared sum of the distances between theoretical and experimental values. When this distance was found to be a minimum in the range considered and within a 95% confidence bound, we chose the final values as the appropriate ones. The real and imaginary parts were also checked separately with the optimization toolbox of Matlab, yielding in all cases good correlation coefficients in the range 0.9−1.

The solution resistance R_s is about 140 Ω. The elements R_f and C_f represent multilayer resistance and capacitance, respectively. Z_d is the diffusion impedance given by eq 1. The inclusion of the resistance R_m in the equivalent circuit accounts for an ohmic conduction mechanism (parallel to diffusion).

When the number of layers becomes very large, the film behaves as a homogeneous membrane, and partitioning effects need to be considered to provide a good account of the experimental observations. The ionic concentration of species k in the vicinity of the multilayer

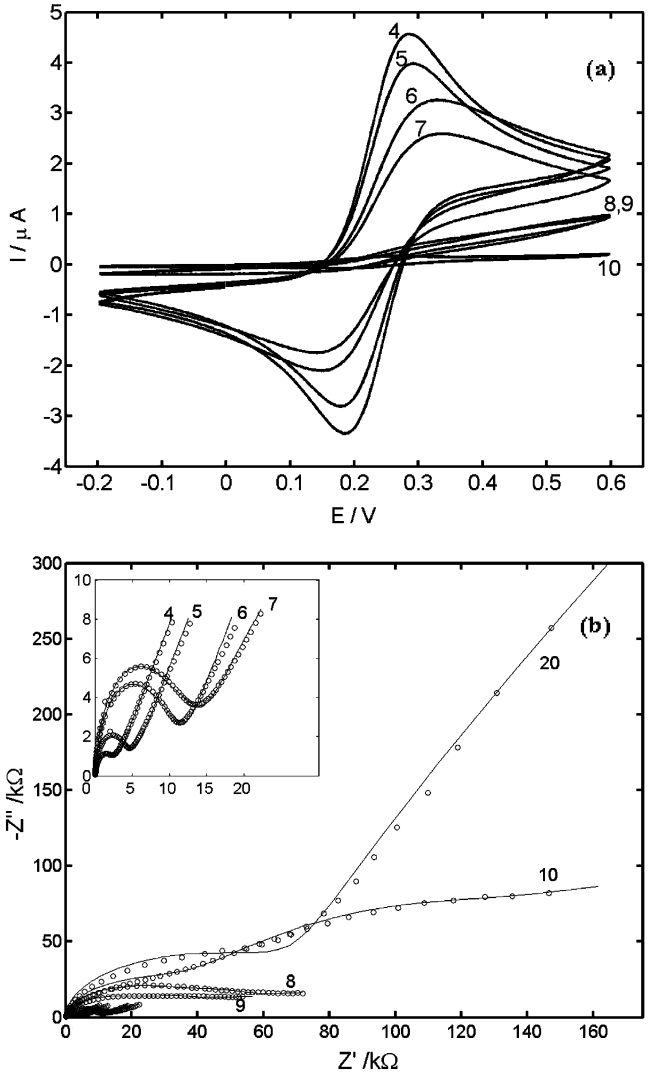

Figure 3. (a) Cyclic voltammograms obtained at 50 mV s^{-1} for gold electrodes modified with a PSS/PAH multilayer in the presence of 0.5 M $NaClO_4$ + $[Fe(CN)_6]^{4-}$ 1 mM + $[Fe(CN)_6]^{3-}$ 1 mM. (b) Impedance spectra of PSS/PAH multilayers and theoretical fittings using the parameter values given in Table 1. The number of layers N is shown near the curves.

surface is then given by $c_k^f = K_k c_k^s$, where c_k^s is its concentration in the bulk solution, and K_k is its partition coefficient. For the sake of simplicity we take $K_1 = K_2 = K$. The apparent charge-transfer resistance is then evaluated as $R_{CT}^{(app)} = R_{CT}/K(1 - \theta)$, where the measured charge-transfer resistance R_{CT} for bare gold was ca. 100 Ω.[19]

4. Results and Discussion

4.1. Influence of the Number of Layers. With an increasing number of layers, the shape of the cyclic voltammograms changes from peak-shaped ($N \leq 7$) to plateau-shaped ($N > 7$), and the current decreases significantly, as shown in Figure 3a. This reflects a change in the geometry of the diffusion field from semi-infinite linear diffusion at a low number of layers to convergent diffusion to an array of microelectrodes as the number of layers increases. Moreover, the reduction in current seems to be related to a lower value of the diffusion coefficient.[19−21] The small increase in peak separation in the CVs with increasing N is attributed to an increase in the film coverage θ, which in turn increases the charge-transfer resistance $R_{CT}^{(app)}$.[19]

The EIS results shown in Figure 3b illustrate more clearly the structural changes. A very large increase in the semicircle diameter and the disappearance of the unit slope line that becomes almost a second semicircle are observed when the number of layers increases. These results are consistent with our previous work, in which three other polycations were studied.[19] It is also seen that the CMM provides very good agreement with the experimental results, having the major advantage over other models of providing information about film properties, such as coverage, average pore radius, and diffusion coefficient. Values for the fitting parameters are presented in Table 1. For $N \leq 7$, a straight line of approximately unit slope is observed at the lowest frequencies, and hence, diffusion is linear in this frequency range. The diagrams for $N > 7$ show a deviation from a straight line of unit slope at low frequencies, indicating nonlinear diffusion. For multilayers with $N > 7$, the diffusion coefficient in the multilayer becomes significantly smaller than that in solution. The "migration resistance" R_m comes also into play, resulting from a more compact structure. For $N = 10$, the difference between the diffusion coefficient in the multilayer and in solution is dramatic, corresponding to a situation where the pinholes are completely covered and the multilayer behaves as an almost homogeneous membrane. This behavior is observed for a PEMU of 20 layers, as seen by the elimination of θ and r_a in the fitting procedure. This last result supports the modeling of a thick PEMU as a homogeneous membrane.[3,19,29−34] When dealing with these thick multilayers with $N = 20$, partitioning of the electrochemical probe ion has to be considered,[32] and the partition equilibrium constant between the multilayer and the solution was estimated to be $K = 0.45$; for all other cases, including all other supporting electrolytes and temperatures, K was always taken to be unity.

The values of the fitting parameters shown in Table 1 evidence that, for $N \leq 9$, the overall trend of the film capacitance C_f is to increase with the number of layers. This reflects that the film area is increasing. The double layer capacitance C_{dl} is constant at this stage. For $N \geq 7$, the geometries to be considered are those of the covered pinholes, and the trends depend strongly on how the internal layers are affected from the deposition of the external ones. This is only significant during the transition to a more compact multilayer. As it should be expected, C_{dl} is always higher than C_f.[19]

The change with N in the high frequency semicircle of the Nyquist diagrams is mainly due to the increase in R_f. It reflects the increase in multilayer thickness and decrease of ion content and mobility, which are associated with film electrical conductivity.[31] The film resistance becomes detectable immediately after the second or third layers, and the values obtained are of the same order of magnitude as those reported by other researchers. In relation to the variation of R_f with N, it is observed that it increases nonlinearly with N. The changes in both coverage θ and radius of the active spots r_a are consistent with the formation of a more compact structure following the addition of every new layer (i.e., the coverage increases and the pore radius decreases with increasing N). These

(29) Decher, G. *Science* **1997**, *277*, 1232.
(30) Diard, J. P.; Glandut, N.; Montella, C.; Sanchez, J.-Y. *J. Electroanal. Chem.* **2005**, *578*, 247.
(31) Durstock, M. F.; Rubner, M. F. *Langmuir* **2001**, *17*, 7865.
(32) Farhat T. R.; Schlenoff, J. B. *Langmuir* **2001**, *17*, 1184.
(33) Rmaile, H. H.; Farhat, T. R.; Schlenoff, J. B. *J. Phys. Chem. B* **2003**, *107*, 14401.
(34) von Klitzing, R.; Tieke, B. *Adv. Polymer Sci.* **2004**, *165*, 177.

Table 1. Parameter Values Obtained by Fitting the Impedance Data of the PSS/PAH Films to the CMM. Uncertainties Are Given for the 95% Confidence Bounds of the Parameter Values

N	C_f (μF)	R_f (kΩ)	C_{dl} (μF)	θ	r_a (μm)	R_m(kΩ)	D_R
4	0.25 ± 0.01	2.0 ± 0.2	1.1 ± 0.2	0.15 ± 0.02	10 ± 1	∞	0.70 ± 0.03
5	0.24 ± 0.01	3.8 ± 0.2	1.1 ± 0.2	0.37 ± 0.02	8.0 ± 0.9	∞	0.70 ± 0.03
6	0.29 ± 0.01	8.8 ± 0.3	1.1 ± 0.2	0.55 ± 0.02	7.9 ± 0.9	∞	0.70 ± 0.02
7	0.29 ± 0.01	10.5 ± 0.5	1.1 ± 0.2	0.45 ± 0.01	8.9 ± 0.9	100 ± 10	0.40 ± 0.02
8	0.30 ± 0.01	38.8 ± 0.9	1.1 ± 0.2	0.34 ± 0.01	7.1 ± 0.8	85 ± 3	0.033 ± 0.003
9	0.295 ± 0.009	26.0 ± 0.9	1.1 ± 0.2	0.32 ± 0.01	6.3 ± 0.8	69 ± 3	0.032 ± 0.003
10	0.24 ± 0.01	48.0 ± 0.9	0.7 ± 0.2	0.35 ± 0.01	4.5 ± 0.6	750 ± 80	0.0046 ± 0.0004
20	0.24 ± 0.01	82.0 ± 0.9	1.6 ± 0.4			∞	0.0046 ± 0.0004

trends are affected, however, for $7 \leq N \leq 10$ layers because of the activation of a new transport mechanism, the migration resistance R_m, which is an alternative path for charge transport. It influences the EIS response just in the transition from a heterogeneous PEMU with cavities to a more compact structure in which the electrode becomes significantly blocked (note that θ becomes an *effective* coverage because of partially covered pinholes when this happens).

The transition from heterogeneous structure to an homogeneous film with increasing number of layers is an agreement with the observations made by Picart and coworkers in AFM pictures of other polyelectrolyte multilayers.[35,36] Those authors showed that the polyelectrolyte deposition begins with the formation of "islands" in the surface. With the increasing number of layers, those islands grow and start to coalesce, and after a certain number of layers, an almost uniform film is observed. These observations support the basic assumptions made in our model for the interpretation of the electrochemical data with increasing number of deposited layers as the formation of the islands reduces the uncovered electrode area and reduces the average diameter of the "pores" between the islands.

4.2. Nature of Supporting Electrolyte. In the presence of an electrolyte solution, it is expected that some small ions enter the multilayer ruled by (Donnan) electrochemical equilibrium.[1] A charge screening effect may also be present, decreasing both the interchain attraction and the intrachain repulsion, similar to the one observed during the preparation of PEMUs in the presence of a salt, when more polyion is needed to totally reverse charge, a necessary condition to grow polyelectrolyte multilayers, creating thicker films.[12,13] In addition, the contact of PEMUs with salt solutions of increasing ionic strength induces partial extrinsic compensation.[11] All these factors contribute to the dissociation of some polyelectrolyte ion pairs, affecting the film structure and reducing the viscosity.[37] This effect was also revealed by the incorporation of barium ions in PEMUs, which was stated to occur via exchange at polyelectrolyte ion pairs.[2] Results obtained with polyelectrolyte complexes point to a decrease in aggregation in the presence of multivalent ions, suggesting an interaction between the multivalent cations and the polyanion.[38] In a previous work[18] where steady-state conditions were considered for charge transport, we also observed that the permeability to a given ion probe is enhanced when considering $Ba(ClO_4)_2$ compared to $NaClO_4$.

In Figure 4, experimental EIS results for Au + cysteamine + $(PSS + PAH)_3$ + PSS in the presence of a 0.1 M concentration of different supporting, $NaClO_4$, $KClO_4$, $Ca(ClO_4)_2$, $Ba(ClO_4)_2$, and $La(ClO_4)_3$, are shown. The theoretical fittings to the equivalent circuit of Figure 2 are also plotted. The parameter values are given in Table 2. It is seen that the impedance decreases for salts with increasingly higher ionic strength. The capillary nonlinear diffusion is present at low frequencies, ruled by the values of θ and r_a, for all electrolytes used, and the amplitude of the semicircle changes significantly at high frequencies, governed by the value of R_f. Within the framework of the CMM, we thus observe that the degree of coverage decreases (and the radius r_a increases) when increasing the valency of the small mobile cations, which theoretically confirms in a compelling manner the previous results mentioned in the above paragraph (interaction between polyelectrolyte chains is lowered, with a higher chance to create loose structures giving place to capillaries). The decreasing value of the film capacitance C_f for increasing valency of the ions is also consistent with the decrease of the coverage. Additionally, because the last layer bears negative charge, a lower value for the film resistance is also to be expected for multivalent cations. Our results confirm this expectation. In the framework of the CMM, we are thus able to interpret the effect of the nature of the electrolyte in terms of a few structural parameters with a well-defined physical meaning. The interaction between small cations and polyelectrolytes was observed to follow approximately the Hofmeister series, as had been presented before for interactions with anions.[39]

Determination of the thickness of four $(PSS + PAH)_3$ films after immersion in different electrolytes was done

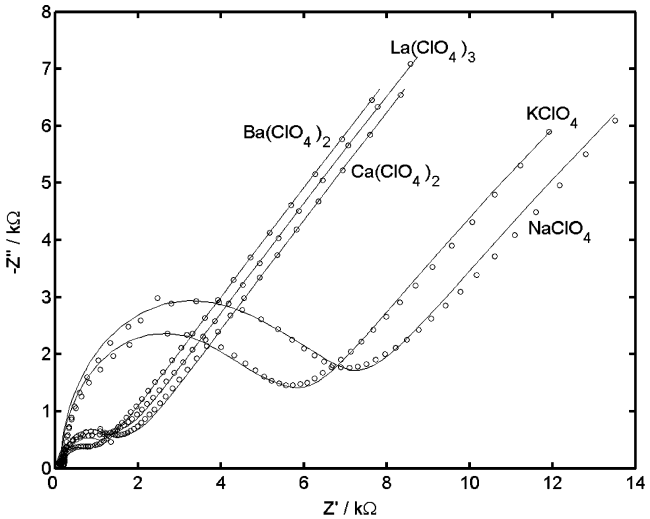

Figure 4. Impedance spectra for a Au + cysteamine + $(PSS + PAH)_3$ + PSS multilayer in the presence of a 0.1 M concentration of supporting: $NaClO_4$, $KClO_4$, $Ca(ClO_4)_2$, $Ba(ClO_4)_2$, and $La(ClO_4)_3$ ($[Fe(CN)_6]^{4-}$ 1 mM and $[Fe(CN)_6]^{3-}$ 1 mM, at formal potential). The theoretical fittings using the parameter values in Table 2 are also shown.

(35) Lavalle, Ph.; Gergely, C.; Cuisinier, F. J. G.; Decher, G.; Schaaf, P.; Voegel, J. C.; Picart, C. *Macromolecules* **2002**, *35*, 4458.
(36) Picart, C.; Lavalle, Ph.; Hubert, P.; Cuisinier, F. J. G.; Decher, G.; Schaaf, P.; Voegel, J. C. *Langmuir* **2001**, *17*, 7414.
(37) Kolaric, B.; Jaeger, W.; von Klitzing, R. *J. Phys. Chem. B* **2000**, *104*, 5096.
(38) Dautzenberg H.; Kriz, J. *Langmuir* **2003**, *19*, 5204.

Table 2. Parameter Values Obtained by Fitting the Impedance Data of the Au + Cysteamine + (PSS + PAH)$_3$ + PSS Film to the CMM for a 0.1 M Concentration of Several Supporting Electrolytes

electrolyte	C_f (μF)	R_f (kΩ)	C_{dl} (μF)	θ	r_a (μm)	R_m(kΩ)	D_R
$NaClO_4$	0.29 ± 0.01	5.5 ± 0.1	1.1 ± 0.2	0.45 ± 0.01	8.2 ± 0.4	100 ± 20	0.85 ± 0.01
$KClO_4$	0.22 ± 0.01	4.5 ± 0.1	1.1 ± 0.2	0.38 ± 0.01	9.9 ± 0.5	100 ± 20	0.95 ± 0.01
$Ca(ClO_4)_2$	0.15 ± 0.01	1.3 ± 0.1	1.1 ± 0.1	0.15 ± 0.01	9.9 ± 0.9	400 ± 90	0.95 ± 0.03
$Ba(ClO_4)_2$	0.15 ± 0.01	0.70 ± 0.05	1.1 ± 0.1	0.15 ± 0.01	9.9 ± 0.9	400 ± 90	0.95 ± 0.03
$La(ClO_4)_3$	0.15 ± 0.01	1.0 ± 0.1	0.9 ± 0.1	0.15 ± 0.02	9.9 ± 0.9	400 ± 90	0.80 ± 0.03

Table 3. Parameter Values Obtained by Fitting the Impedance Data of the Au + Cysteamine + (PSS + PAH)$_3$ + PSS Film to the CMM for Different Temperatures

T(°C)	C_f(μF)	R_f (kΩ)	C_{dl} (μF)	θ	r_a (μm)	R_m(kΩ)	D_R
15	0.40 ± 0.01	17.2 ± 0.1	1.1 ± 0.2	0.43 ± 0.02	8.9 ± 0.8	140 ± 40	0.13 ± 0.01
25	0.40 ± 0.01	15.5 ± 0.1	1.1 ± 0.2	0.45 ± 0.01	8.9 ± 0.7	125 ± 30	0.28 ± 0.02
35	0.40 ± 0.01	12.5 ± 0.1	1.1 ± 0.1	0.45 ± 0.01	8.9 ± 0.8	300 ± 90	0.47 ± 0.01
45	0.46 ± 0.01	8.5 ± 0.1	1.1 ± 0.1	0.45 ± 0.01	8.9 ± 0.8	300 ± 90	0.62 ± 0.01

to further evaluate the effect of small ions on the structure of the polyelectrolyte films. The ellipsometry of "dry" films demonstrates that the spatial variation of the film thickness has the same magnitude of the differences between the averages for each film: immersion in $NaNO_3$ 0.1 M, $d = 5 \pm 1$ nm; after immersion in KNO_3 0.1 M: $d = 5 \pm 2$ nm; after immersion in $Ca(NO_3)_2$ 0.1 M: $d = 5.2 \pm 0.4$ nm; after immersion in $Ba(NO_3)_2$ 0.1 M, $d = 4.8 \pm 0.5$ nm. The structural changes pointed due to the interaction with small ions are thus not revealed in the film thickness, but mainly in changes of the entanglement of the polyelectrolyte chains. Consistent with previous studies,[40,41] a smaller variation is observed for the films immersed in electrolytes with divalent cations, i.e., higher ionic strength, meaning that these films have a lower roughness.

4.3. Temperature. The response to temperature changes is an important issue for the application of polyelectrolyte multilayered films. The structure of the multilayer results from a competition between the disordering effect of entropy and the ordering effect of the electrostatic interactions among polyelectrolyte chains. A moderate temperature increase enhances the role of entropy, and the structure becomes looser. Thus, although the stability of the multilayer could be not affected on average, an enhanced diffusion of small mobile species is to be expected with increasing temperature.

The temperature effects on a Au + cysteamine + (PSS + PAH)$_3$ + PSS modified electrode have been studied by CV and EIS, and the results are shown in Figure 5, parts a and b. At 15 °C, the CVs are broad, nearly plateau-shaped, suggesting a lower diffusion coefficient through the PEMU. With increasing temperature, the CVs become more peak-shaped and show larger peak currents. The EIS spectra in Figure 5b show a significant reduction in impedance with increasing temperature. The parameter values fitting the experimental results are tabulated in Table 3. They reveal an increase in the diffusion coefficient in the multilayer and a decrease in the film resistance with increasing temperature, while the coverage and pore radius remain constant. This physical picture of the temperature effects thus provided by the CMM is consistent with a previous experimental work in which the changes in conductivity were ascribed to changes in mobility and effective concentration of small ions in the film.[31] Moreover, as it is shown in Figure 6, the change of the diffusion coefficient with temperature follows the Arrhenius law

$$\ln D^f = \ln A - \frac{E_a}{RT} \quad (5)$$

where A is the preexponential Arrhenius factor and E_a is the activation energy. By fitting the results to this

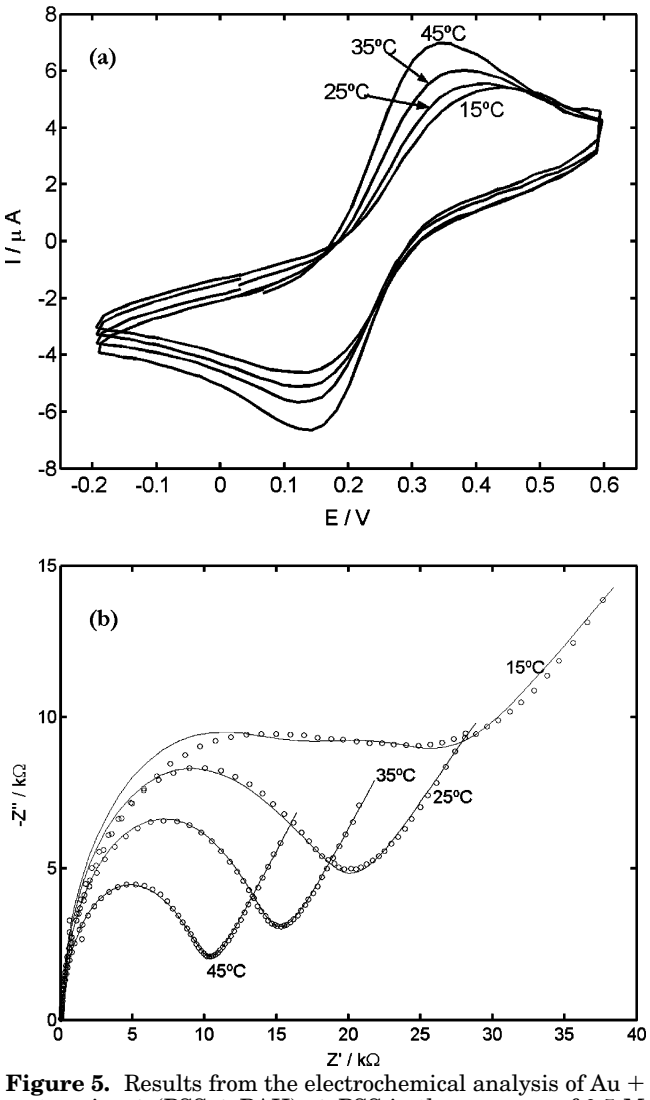

Figure 5. Results from the electrochemical analysis of Au + cysteamine + (PSS + PAH)$_3$ + PSS in the presence of 0.5 M $NaClO_4$ + $[Fe(CN)_6]^{4-}$ 1 mM + $[Fe(CN)_6]^{3-}$ 1 mM, at different temperatures: (a) Cyclic voltammograms obtained at 50 mV s^{-1}; (b) Experimental EIS results and theoretical fittings using the parameter values in Table 3.

(39) Salomäki, M.; Tervasmäki, P.; Areva, S.; Kankare, J. *Langmuir* **2004**, *20*, 3679.
(40) Dubas, S. T.; Schlenoff, J. B. *Langmuir* **2001**, *17*, 7725.
(41) McAloney, R. A.; Dudnik, V.; Goh, M. C. *Langmuir* **2003**, *19*, 3947.

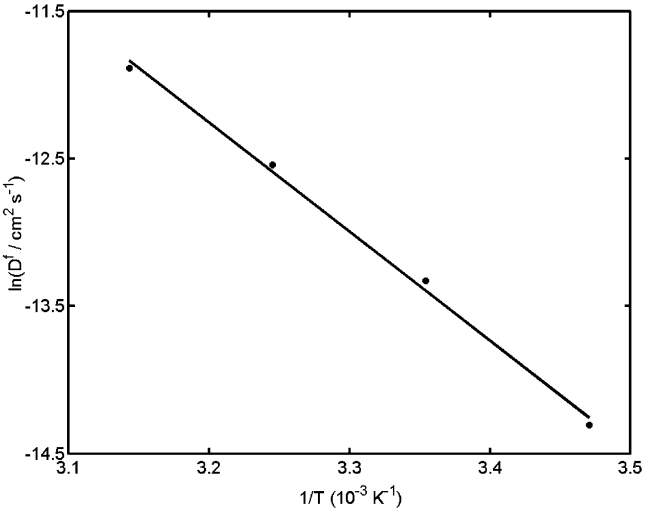

Figure 6. Logarithmic plot of the diffusion coefficient in the film against the reciprocal absolute temperature.

equation, we obtain $A = 8.76 \times 10^4$ cm^2 s^{-1} and $E_a = 61.4$ kJ/mol. This activation energy is similar to that obtained for the self-diffusion of polymers.[42]

5. Conclusions

The ability of the CMM to explain the EIS response of PEMUs has been confirmed for a different PEMU consisting of PSS as polyanion and PAH as polycation at different stages of its building-up process. We have studied also here thicker PEMUs that are almost homogeneous. The CMM has been used to fit EIS measurements, and a number of effects have been explained theoretically, specifically, the influence of the valency of the ionic species and temperature on the permeability and the changes in EIS response depending on the number of layers of the multilayer. We find that structural changes taking place can be described in terms of coverage of the electrode and radius of the opened paths for charge transport. The former tends to increase and the latter decreases as the number of layers increases. The effect of the nature of the supporting electrolyte is interpreted in terms of structural changes described by the film resistance, coverage, and radius of the active spots for diffusion. It is shown that the coverage and film resistance is generally lower (the radius of active sites being larger) for PEMUs in contact with electrolyte solutions containing multivalent ions compared to monovalent ones. This is due to a stronger interaction between the multivalent ions and the polyelectrolyte chains, competing with the complexation and thus favoring the opening of paths for charge transport. Finally, the effect of increasing temperature on the EIS response is interpreted as a change in the diffusion coefficient following the Arrhenius law, together with a decrease in the film resistance that is consistent with the induced disorder in the PEMU favoring the mobility of ionic species.

Acknowledgment. Financial support from the Fundação para a Ciência e a Tecnologia (FCT) CIQ-L4, from the CICYT (Ministry of Science and Technology of Spain) and FEDER (European Funds for Regional Development) under project No. MAT2002-0646, and from the European Union under the research and training network SUSANA (HPRN-CT-2002-00185) is gratefully acknowledged. T. H. Silva also acknowledges FCT for a Ph.D. grant. The authors wish to acknowledge Dr. Rui Azevedo for his assistance during the ellipsometric measurements at the Instituto de Engenharia Biomédica (INEB), Porto.

LA0507176

(42) Vartapetian, R. S.; Khozina, E. V.; Karger, J.; Geschke, D.; Rittig, F.; Feldstein, M. M.; Chalykh, A. E. *Colloid Polym. Sci.* **2001**, *279*, 532.